

Revision 1. Crystal chemistry of Cu-bearing tourmalines

O.S. Vereshchagin^{1,*}, I.V. Rozhdestvenskaya¹,
O.V. Frank-Kamenetskaya¹, A.A. Zolotarev¹, R. I. Mashkovtsev²
¹ Saint-Petersburg State University, Saint Petersburg, Russia
² VS Sobolev Institute of Geology and Mineralogy SB RAS.

*Present address: Department of Mineralogy, Saint Petersburg State University, Universitetskaya nab.
7/9 Saint Petersburg, 199034, Russia. E-mail: oleg-vereschagin@yandex.ru

Abstract

The crystal structures of two elbaïtes from the Paraiba deposit with copper contents of 3.51 and 1.61 wt. % CuO ($a=15.881(1)$, $15.840(3)$; $c=7.112(1)$, $7.1028(9)$, respectively), as well as a synthetic Cu-bearing olenite with CuO content 8.39 wt.% ($a=15.840(4)$, $c=7.091(1)$) have been refined to R-indices of 2.2, 3.1 and 4.1 % using X-ray single-crystal method. On the basis of original and published data (for six structures) the crystal-chemical relationships of copper-bearing tourmalines were analyzed. It was shown that copper cations and cations of other 3d elements (Mn, Zn, Fe) almost occupy only Y site. Such ordered distribution results in a change in size of the Y-octahedra. There is an inverse correlation between the content of 3d elements (firstly Cu^{2+} cations) and Al^{3+} cations in the Y-octahedron and also between the value of $\langle\text{Y-O}\rangle$ and the content of Al^{3+} cations in the Y site. The direct correlation between values of $\langle\text{Y-O}\rangle$ -distance in the structures of Cu-bearing elbaïtes and the parameters (a , c) of the unit cell have been found. Distortions of polyhedra in the structures of Cu-bearing elbaïtes are similar, and significantly higher than those present in the structure of the synthetic Cu-bearing olenite.

Keywords: Cu-rich elbaïte, Cu-bearing olenite, Paraiba, crystal chemistry, tourmaline, X-ray structure refinement

Introduction

Copper ions in a tourmaline were first found (in the ppm range) in the middle of the 20th century in occurrences in Tanganyika and South-West England (Bassett et al., 1953; Power et al., 1968). The first traces of tourmaline with a concentration of CuO up to 2 wt. % were found in 1980s in the Batalha occurrence, state of Paraiba, northern Brazil (Koivula and Kammerling, 1989; Bank et al., 1990). Tourmalines found in this deposit were sapphire-blue, neon-blue, indigo, or bluish-violet in color, and were valuable jewelry materials. The price for some samples was higher than \$ 20.000/ct. At the present time, copper-bearing elbaïtes are also found in Namibia: the Khan pegmatite close to Rossing (Haughton et al., 1969); Nigeria: the Edeko mine near Ilorin in the state of Ojo (Zang and Da Fonseca-Zang, 2001) and in the occurrence situated near Alto Ligonha, Mozambique (Abduriyim et al., 2006; Laurs et al. 2008).

39 Synthetic copper-bearing tourmalines were first produced by I.E. Voskresenskaya at the Institute
40 of Crystallography of the USSR Academy of Sciences (AS) (Voskresenskaya, 1968). The largest
41 tourmaline crystals, which reached a size of 1–2 mm, with up to 14 wt. % CuO, were synthesized at the
42 Institute of Mineralogy and Petrography, Siberian Branch (SB) of Academy of Sciences, Novosibirsk
43 (Lebedev et al., 1988).

44 Over the past thirty years, Cu bearing tourmalines have been the subject of several dozen articles,
45 most of which have been related to their unique jewelry properties, the features of their chemical
46 composition, and geological conditions of their occurrence (Koivula et al., 1989; Shigley et al., 2001;
47 Wilson, 2002; Abduriyim et al., 2006; Breeding et al., 2007; Furuya & Furuya, 2007, etc.).

48 The crystal chemistry of copper-bearing tourmaline has received less attention. To date, there
49 exists data on just three refinements of tourmaline crystal structures, which contain less than 1 wt. % CuO
50 (MacDonald & Hawthorne, 1995; Ertl et al., 2002).

51 The aim of our work was to define the crystal structures of three tourmalines with different copper
52 contents, and analyze the crystal chemistry of copper bearing tourmalines on the basis of original and
53 published data.

54

55 ***Materials and methods***

56

57 Two natural and one synthetic tourmaline with different copper contents were chosen for research
58 (Table 1).

59 Synthetic tourmaline (Sample 1) was grown in the Institute of Mineralogy and Petrography AS,
60 in Novosibirsk. Synthesis was conducted by the hydrothermal method at a temperature of 650 °C and a
61 pressure of 1.5 kbar in solutions 0.05 (H, Na) - 0.05 H₃BO₃-0.9 H₂O (mole fraction). Mixture
62 consisting of powdered Al₂O₃, α-quartz (fraction 1-2 mm) and copper oxide was used. The Al/Si/Cu
63 mole ratio was about 1/1/0.3, the solution/solid molar ratio about 25. The tourmalines were grown on
64 seed plates of natural tourmaline (size 5x2x1 mm, the composition of the seed is close to pure elbaite),
65 placed between the silica source (above) and alumina source (below), in sealed gold tubes (V= 150
66 cm³). The charged gold tube and pure water as a pressure medium were filled and enclosed in a
67 Bridgman type steel vessel with capacity of 200 cm³ and then heated during 30 days. Total variations
68 and uncertainty were estimated as ±10 °C in temperature and ±0.1 kbar in pressure (Taran et al., 1993,
69 Lebedev et al., 1988).

70 Both of the natural Cu-bearing elbaite studied (Samples 2 and 3) were found in the State of
71 Paraíba, Brazil. The Paraíba tourmalines occur in northeastern Brazil in four deposits of highly
72 fractionated and zoned granitic pegmatites of the Borborema Pegmatitic Province. “The Borborema
73 Pegmatitic Province covers an area of 150×75 km² in the eastern part of the NNE-striking Seridó

74 Foldbelt in the Northern Domain of the Borborema Tectonic Province. Paraíba tourmaline bearing
75 pegmatites are rich in spodumene or lepidolite, and are emplaced in iron-poor quartzites or
76 metaconglomerates of the Neoproterozoic Equador Formation. The Paraíba tourmaline occurs at the
77 transition between the albite-rich inner intermediate zone and the quartz core of the pegmatites, in
78 primary wedge-shaped crystals of near-end-member color-zoned elbaite, arranged in fan-like, radial or
79 comb-textured groups of crystals. This color-zoned tourmaline most commonly forms the intermediate
80 growth-zone of color-zoned elbaite crystals having a pink to red core and a green to dark green rind”
81 (Beurlen H. et al., 2011)

82 **Chemical studies**

83 The elemental compositions of all single crystals used for the refinement of crystal structure
84 were analyzed with a wavelength-dispersive Link AN-10000 using an automated CamScan 4-DV
85 electron microprobe at the V.G. Khlopin Radium Institute (analyst Yu.L. Kretser). The conditions of
86 the experiment were: accelerating voltage - 20 kV, beam current- 4 nA, data collection time - 60 sec
87 (excluding dead time). The following standards for $K\alpha$ X-ray lines were used: Na - albite, K -
88 orthoclase, Ca – diopside, Si - almandine, Al - kyanite, Ti – rutile, Fe – iron, Mn - manganese; Zn -
89 zinc; Mg – augite, Cu-copper. The fluorine content was analyzed with a wavelength-dispersive INCA
90 Energy 450 using an automated CamScan MX2500 electron microprobe at the VSEGEI (analyst A.V.
91 Antonov). Each grain was analyzed at a minimum of 15 points to obtain good counting statistics.

92 Calculations of preliminary crystal-chemical formulas on the basis of microprobe analysis data
93 were carried out on 15 cations (Zolotarev et al., 2007). In Samples 2 and 3, Li being estimated by
94 iteration as 49 minus ($O_{18}(BO_3)_3V_3W$), suggesting that the V and W positions were only populated by
95 monovalent anions (OH, F) (Burns et al. 1994, Henry & Dutrow 1996). The copper valence was
96 determined by the Electron paramagnetic resonance (EPR) method. The EPR spectra were recorded on
97 a Radiopan SE/X 2543 spectrometer, with a working frequency of about 9.3 GHz. To determine the g-
98 factor and spin amount, a powdered sample of 2,2'-diphenyl-1-picrylhydrazyl (DPPH) with $g = 2.0036$
99 was used.

100 **Crystal structure refinement**

101 X-ray data collection was carried out with X-ray single-crystal automatic diffractometers (Table 2)
102 in one-sixth of the reciprocal space (Samples 1 and 3) and a full sphere (Sample 2) using $MoK\alpha$ radiation
103 ($\lambda = 0.71073 \text{ \AA}$).

104 The intensities were corrected for Lorentz and polarization factors. The refinement of crystal
105 structures was carried out in a space group typical for tourmalines, $R3m$, on the basis of unequivalent
106 reflections with $F > 4\sigma F$, alternating least squares (taking into account the anisotropy of the displacement
107 parameters of atoms), and analysis of difference Fourier syntheses by means of the CSD software package
108 (Akselrud et al., 1989). The coordinates of atoms in the structure of aluminum-rich elbaite (Gorskaya et

109 al., 1982) were used as initial conditions. Aluminum atoms were placed at Y and Z octahedral sites, and
110 sodium atom was positioned at the alkali cation site. X-ray scattering at these sites was actually
111 determined by refining the occupancies on the basis of the small-angle reflections ($\text{Sin}\theta/\lambda \leq 0.5$) that are
112 slightly affected by uncertainties in temperature factors. The absorption correction was made with
113 program DIFABS (Walker and Stuart, 1983), after refinement of the anisotropy displacement parameters
114 of the atoms.

115 After the crystal structure refinement, a procedure of cation distribution optimization over
116 crystallographic sites was performed by minimizing the differences between the results of chemical
117 analysis, the scattering of the cation sites, bond lengths and valence balance (Wright, 2000). The
118 optimized formula minimizes the differences between the formula obtained by chemical analysis and that
119 obtained by structure refinement. The coefficients in the final crystal-chemical formula were obtained
120 from chemical analysis, site scattering, and bond-lengths. The final lithium contents of Samples 2 and 3
121 were calculated from site scattering, site bond-lengths, and balance of charges, with the use of flame-
122 photometry data.

123 **Chemical deformations**

124 The chemical deformations of Cu-bearing tourmaline structures studied and described in the
125 literature were analyzed on the basis of variations of the unit cell constants and the sizes of the polyhedra.
126 Polyhedra distortions were estimated using equations (Ertl et al., 2002):

$$\Delta X = \frac{1}{9} \sum_{i=1}^9 \left[\frac{(X-O)_i - \langle X-O \rangle}{\langle X-O \rangle} \right]^2; \quad \Delta_{\text{oct}} Z = \frac{1}{6} \sum_{i=1}^6 \left[\frac{(Z-O)_i - \langle Z-O \rangle}{\langle Z-O \rangle} \right]^2;$$
$$\Delta_{\text{oct}} Y = \frac{1}{6} \sum_{i=1}^6 \left[\frac{(Y-O)_i - \langle Y-O \rangle}{\langle Y-O \rangle} \right]^2; \quad \Delta T = \frac{1}{4} \sum_{i=1}^4 \left[\frac{(T-O)_i - \langle T-O \rangle}{\langle T-O \rangle} \right]^2.$$

127

128 **Results**

129

130 **Chemical composition**

131 The copper content of the investigated tourmalines varied from 0.17 to 1.08 apfu (from 1.46 to
132 8.39 wt. % CuO, respectively, Table 3), which is much greater than the content of the element in
133 previously structure studied samples (MacDonald & Hawthorne, 1995; Ertl et al., 2002). The elemental
134 composition of the natural tourmalines investigated (Samples 2 and 3) is typical for elbaïtes from the
135 Paraiba occurrence, Brazil (Table 4) and is much more diversified than the synthetic tourmaline (Sample
136 1). For all samples studied, the main cation in the X-site was Na^+ . In natural samples, a trace of calcium
137 and significant part of vacancy was also found in that site. In addition, in all cases the content of Al^{3+} was
138 greater than 6 apfu, which indicated this cation was not only present in Z-octahedra. The content of Al^{3+}
139 cations in the synthetic tourmaline reaches 7.92 apfu, which indicates it is as a synthetic analog of olenite
140 according to the tourmaline nomenclature (Henry et al., 2011). In the composition of elbaïtes, besides Cu

141 cations, other 3d element cations (Mn, Zn and Fe) were also found at trace levels (from 0.03 to 0.27 apfu).
142 Another important feature of the studied tourmalines' chemical composition was a low silica content
143 (which also evident in variation of the Si / Al ratio). In the synthetic sample the Si content equals 5.26
144 apfu, compared to natural samples, where it varies from 5.87 to 5.93 apfu (Table 3). Both natural
145 tourmalines contain relatively low amounts of F (Table 3).

146 **EPR-data**

147 The central EPR spectrum of the synthetic tourmaline (Sample 1) consisted of four poorly
148 resolved lines of hyperfine structure at $g_c = 2.021$, with splitting between the two central lines similar to
149 9.3 mT, the line width between inflexion points $\Delta H_{pp} \sim 7$ mT. In previous work (Bank & Henn, 1990;
150 Rossman et al. 1991) it has been shown that such spectra are related to the Cu^{2+} ion, and the magnetic
151 parameters (principal values and principal directions of \mathbf{g} and \mathbf{A} matrices) of the EPR spectrum were
152 determined to be due to narrow EPR lines ($\Delta H_{pp} \approx 1.5$ mT) observed in African elbaite with a low copper
153 content. The magnetic parameters suggest that Cu^{2+} ions enter elongated Y-octahedra (Mashkovtsev et al.,
154 2006).

155 **X-ray single crystal analysis data**

156 The results of X-ray studies (Tables 5-7) confirmed that the X-site cation of the investigated
157 tourmalines was Na^+ , which reached 0.86 apfu (Sample 1). The content of Ca^{2+} ions in the natural samples
158 2 and 3 was ≤ 0.1 apfu. The X site was partly vacant in all the investigated samples.

159 In the synthetic tourmaline (Sample 1) the experimental value $\langle \text{Y-O} \rangle = 1.978(6)$ Å within the
160 standard deviation matched the calculated value of $\langle \text{Y-O} \rangle = 1.972$ Å for the content of the Y site
161 ($\text{Al}_{0.62}\text{Cu}_{0.38}^{2+}$), obtained as a result of site scattering. The size of that octahedron is smaller in comparison
162 to the size of the octahedron (1.992 Å) in the structure of Fe-bearing olenite
163 ($\text{Na}_{0.54}\text{Ca}_{0.14}\text{K}_{0.01}\square_{0.31})(\text{Al}_{2.15}\text{Fe}_{0.78}^{2+}\text{Mn}_{0.06}^{2+}\text{Ti}_{0.01}^{4+})(\text{Al}_{5.90}\text{Mg}_{0.10})(\text{Si}_{5.60}\text{Al}_{0.40})\text{B}_3\text{O}_{27}(\text{OH})_{2.49}\text{O}_{0.51}$
164 ($\text{O}_{0.99}\text{F}_{0.01}$) (Cempirek et al., 2006). This fact is associated with the presence of large Fe^{2+} cations in the
165 Y-octahedron. The mean bond distance of Z octahedron $\langle \text{Z-O} \rangle$ is 1.907(5) Å. Taking into account the
166 site scattering of Z site we suggest the Cu-cation share less than ~ 0.1 apfu. It should be mentioned that
167 such a concentration of copper in the Z position is close to the within the possible definition of this
168 method. The length of the bond (Y-O3) was 2.123 Å, which is significantly longer than (Y-W1(O1)) =
169 1.958 Å, and confirmed that the O3 site is occupied by $(\text{OH})^-$ and the W1(O1) site by oxygen. This is
170 in good agreement with the assumption of Hawthorne (2002): "about occupancies O3 and O1 sites in
171 olenite as $^{\text{O}3}[\text{O}_2(\text{OH})]^{\text{O}1}(\text{O})$, because the strength of the hydrogen bond involving OH at O3 is stronger
172 than the strength of the hydrogen bond involving OH at the O1 site".

173 In the natural elbaite studied (Samples 2 and 3), in addition to Cu cations (atomic number 29),
174 Mn cations (atomic number 25) were also found (Table 3). In Sample 3 cations of Zn (atomic number
175 30) and Fe (atomic number 26) were also present. These 3d-elements (Cu, Zn, Mn, Fe) are similar not

176 only in their scattering power, but also in size: $r_{\text{Cu}^{2+}} \cong r_{\text{Zn}^{2+}}$ (0.73, 0.74 Å, respectively), $r_{\text{Fe}^{2+}} \cong r_{\text{Mn}^{2+}}$
177 (0.78, 0.81 Å, respectively) (Bosi et al., 2007). The results of defining the scattering sites and
178 analyzing the bond lengths (Tables 5 and 6) showed an admixture of heavy elements (compared to Al
179 and Li) in both octahedral sites (in proportions similar to those for the synthetic olenit). Taking into
180 account that Mn^{2+} cations normally occupy the Y site (according to structural studies of Mn-containing
181 tourmaline (Burns et al., 1994; Ertl et al., 2003)), we can assume these cations also occupy only the Y
182 site in studied natural tourmalines (Table 5). The experimental value of $\langle \text{Y-O} \rangle = 2.024(6)$ Å for the
183 crystal structure of Sample 2 is in good agreement with the calculated value of $\langle \text{Y-O} \rangle = 2.022$ Å for
184 the composition of the Y site ($\text{Al}_{0.50}\text{Li}_{0.25}[\text{Cu,Zn}]_{0.18}\text{Mn}_{0.06}\text{Fe}_{0.01}$) obtained from the scattering power of
185 the site. The composition of that site, which is occupied by the large cations Cu^{2+} , Zn^{2+} , and Li^+ , as
186 well as even larger Mn^{2+} cations, significantly increases the size of this octahedron, compared to the
187 size of the Y-octahedron (1.978 Å) in the structure of the synthetic Cu-containing tourmaline (Sample
188 1). It is comparable in size to the Y-octahedron (2.022 Å) in the structure of elbaite with Y site
189 composition ($\text{Li}_{0.52}\text{Al}_{0.48}$) (Rozhdestvenskaya et al., 2005). In Sample 3 the experimental value for the
190 Y-octahedron ($\langle \text{Y-O} \rangle = 1.999(4)$ Å) within one esd is also in good agreement with the calculated
191 value of $\langle \text{Y-O} \rangle = 2.000$ Å for the composition of the Y site ($\text{Al}_{0.54}\text{Li}_{0.36}\text{Mn}_{0.10}$), obtained from the
192 scattering power. A significant portion of this site (0.54 atoms) is occupied by trivalent Al^{3+} cations.
193 Another 0.46 atoms per site are occupied by the cations Li^+ or Mn^{2+} , which result to a decrease in the
194 size of this octahedron compared to the Y-octahedron in the structure of elbaite (2.022 Å)
195 (Rozhdestvenskaya et al., 2005). In both elbaites the real bond length $\langle \text{Z-O} \rangle = 1.906(2)$ Å, taking into
196 account the site scattering of Z site, which corresponds to the following composition $\text{Al}_{0.95}[\text{Cu,Zn}]_{0.05}$
197 and $\text{Al}_{0.97}\text{Cu}_{0.03}$ for Samples 2 and 3, respectively. Such a slight increase of the $\langle \text{Z-O} \rangle$ -distance (by
198 1.907(5) Å) which has already been found earlier in copper-free elbaite (Rozhdestvenskaya et al.,
199 2005) can be explained by a positive correlation between $\langle \text{X-O} \rangle$ and $\langle \text{Z-O} \rangle$ distances due to inductive
200 effects in the structure (Ertl & Tillmanns, 2012). Overall, analysis of the cations distribution in natural
201 copper-containing tourmalines (Samples 2 and 3) showed that aluminum is a major element in the Y-
202 and Z-octahedra.

203 In two case, sizes of tetrahedra ($\langle \text{T-O} \rangle = 1.625, 1.621$ Å for samples 1 and 2) exceed the distance
204 characteristic of a tetrahedron, which is fully occupied by Si (~1.620 Å, MacDonald and Hawthorne 1995;
205 Hawthorne 1996; Ertl et al. 2010), which points to entry of a larger cation. It should be Al^{3+} cations based
206 on the data of chemical analysis. The site scattering data shows that this site is occupied by lighter cation
207 (Al or B). If we assume the absence of boron cations, the percentage of aluminum in the T-position will be
208 0.60, 0.32, 0.30 apfu for sample 1, 2, 3 respectively. The total assigned Al content is consistent with the
209 chemical data (Table 3). Thus we assume that the amount of $^{[4]}\text{B}$ in the investigated tourmalines is

210 relatively small, if present. Accurate data would have been necessary to estimate the T-site occupation in
211 detail.

212 The average bond length in the boron triangle of all the investigated samples is almost the same
213 ($\langle B-O \rangle = 1.375, 1.373 \text{ \AA}$), suggesting that the B-site is occupied by boron ($\langle B-O \rangle = 1.376$, Bosi et al.,
214 2004.)

215 As is known, the tendency for orderly distribution of OH^- and F^- ions leads the W1(O1) site to split
216 in the elbaite structure (Rozhdestvenskaya et al., 2005). In the crystal structures of the natural elbaite
217 investigated (Samples 2 and 3), the W1(O1) site is also split into two partially occupied sites, namely, the
218 W1 threefold site and the W2 ninefold site (Table 5). Each atom (vacancy) at the W1 site (on the threefold
219 axis) is surrounded by three corresponding structural units at the W2 sites. The total occupancy of this
220 grouping is 0.94 and 1.00 for Samples 2 and 3, respectively. As a consequence, the following are the
221 shortest forbidden distances appearing in the structures: $W1-W2 = 0.50(3)$ and $0.44(3) \text{ \AA}$ and $W2-W2$
222 $= 0.85(5)$ and $0.72(4) \text{ \AA}$ (for Samples 2 and 3, respectively). In both structures, the Y-W2 bond lengths are
223 approximately equal to $1.70-1.74 \text{ \AA}$ (Table 6). This suggests that the W2 sites are statistically occupied by
224 fluorine anions. The above assumption is confirmed by the fact that the fluorine contents determined by
225 chemical analysis of Samples 2 and 3 (0.24 and 0.28 apfu) are close to those calculated from the
226 occupancies of the W2 site (0.16 and 0.18 apfu).

227 The final crystal-chemical formulas of the tourmalines examined (Table 7) are in good agreement
228 with those calculated from the chemical analysis data (Table 3).

229

230 ***Crystal chemistry peculiarities of copper bearing tourmalines***

231

232 The copper content of the Cu-bearing tourmalines studied and described in the literature (Table
233 7) ranges from 0.38 to 8.39 wt.% CuO (0.05 to 1.26 apfu). All natural Cu-bearing elbaite (No 1-6)
234 also contain cations of other 3d elements (Zn, Mn and Fe). Copper and other 3d elements cations almost
235 only occupy Y octahedron. Their content in it varies from 0.13 to 1.14 apfu. Such ordering distribution of
236 copper cations is well explained by the Goldschmidt rule, characterizing the closeness of the ionic radii
237 of elements that replace each other (Goldschmidt, 1933). In the case of ideal elbaite, the differences
238 between the ionic radii of copper cations, and cations occupying Y- octahedra ($Al_{0.5}Li_{0.5}$) and Z-
239 octahedra ($Al_{1.0}$), is 11 and 25 %, respectively. The content of 3d elements in the Z site, as estimated by
240 crystal structure refinement, is very small (0.12 – 0.19 apfu), and is independent of the overall copper
241 content.

242 In a synthetic olenite (No 1, Table 7), compensation for charge imbalances arising while
243 exchanging a portion of the Al^{3+} for Cu^{2+} cations is provided by the appearance of vacancies in the X-
244 site, and the replacement of oxygen atoms in the V-site for $(OH)^-$ anions according to the equation:

245 ${}^X\text{Na}^{+}+{}^Y, Z\text{Al}^{3+}+2{}^V\text{O}^{2-} \leftarrow {}^X\text{Cu}^{2+}+2{}^V\text{OH}^{-}$. In the structures of the elbaïtes analyzed, as the copper
246 content rises, then the Al and Li content in the Y site, and the number of vacancies in the X-site, both
247 decrease. Al^{3+} cations partly redistribute from octahedral to tetrahedral sites. The charge balance is
248 retained according to the equation: ${}^X\text{Si}^{4+}+{}^Y\text{Li}^{+}+{}^Y, Z\text{Al}^{3+} \leftarrow {}^X\text{Na}^{+}+{}^T\text{Al}^{3+}+2{}^Y, Z\text{Cu}^{2+}$. As the content of
249 Cu^{2+} cations increases, the fluorine content also decreases insignificantly. There is an inverse correlation
250 between the content of 3d elements and Al^{3+} cations in the Y-octahedron ($r = -0.94$, P (probability)
251 $=0.98$, Fig. 1a). The existence of this inverse correlation between copper content and Al^{3+} cations in the
252 Y site ($r = -0.95$, $P = 0.99$, Fig. 1b) is well explained by preferential localization of Cu^{2+} cations in this
253 site.

254 The size of the Y-octahedron is the most variable parameter in the structure of copper-bearing
255 tourmalines: the range of $\langle\text{Y-O}\rangle$ varied from 1.987 to 2.024 Å (Table 8). This is the result of significant
256 variations in their compositions (Table 6). For elbaïtes (No 2–6, Tables 7, 8), there is a direct
257 correlation between the average size of the Y-octahedron $\langle\text{Y-O}\rangle$ and overall content of Cu^{2+} cations (r
258 $= 0.99$, $P = 0.99$; Fig 2a,) as well as the content of 3d elements in the Y site ($r = 0.98$, $P = 0.99$). There is
259 an inverse correlation ($r = -0.98$, $P = 0.99$; Fig. 2b) between the value of $\langle\text{Y-O}\rangle$ and the content of Al^{3+}
260 cations in the Y site. This is well explained by the earlier mentioned correlation between the content of Y
261 site occupying elements for all the investigated tourmalines. Values for the size of $\langle\text{Y-O}\rangle$ in the structures
262 mentioned (2.022, 1.978 Å, respectively) are well explained by the ratio between Al^{3+} / another large
263 cation (Li^{+} or Cu^{2+}) (Table 7).

264 The variations in the average size of the Z-octahedron ($\langle\text{Z-O}\rangle = 1.903\text{--}1.907$ Å) are insignificant
265 and this is due to the fact that they are characterized by almost unchangeable content (mostly occupied by
266 Al).

267 There is a direct correlation between values of $\langle\text{Y-O}\rangle$ -distance in the structures of Cu-bearing
268 elbaïtes (No 2-7, Table 7, 8) and the parameters of the unit cell (Fig. 3). Such a dependency has already
269 been mentioned for elbaïte (Bosi et al., 2005).

270 Values of the $\langle\text{T-O}\rangle$ -distance in copper-bearing tourmalines (No 1– 6, Tables 7, 8) vary from
271 1.616 to 1.625 Å. As was shown before the increasing $\langle\text{T-O}\rangle$ -distance in some cases (No 1-3, Table 8)
272 can be explained by the entry of Al^{3+} cations (by 0.60 apfu). Ertl et al. (2002) suggested that the T sites of
273 a Cu-bearing elbaïte (No 4, Table 8) partially occupied by B cations, (0.26 apfu), which should lead to
274 reduction in the size of the tetrahedron.

275 The values of the bond-angle polyhedra distortions in Cu-bearing tourmalines increase according
276 to: T site \langle Z site \langle Y site \langle X site. This is typical for the entire tourmaline group, and well explained by
277 the polyhedral coordination number and its mixed occupation by cations of different sizes (Ertl et al.,
278 2002). The distortions ΔX and $\Delta_{\text{oct}} Y$ in structures of F-bearing elbaïtes (No 2-7, Table 7, 8) are close to
279 each other, and significantly higher than in the structure of the Cu-bearing synthetic olenite (No 1, Tables

280 7, 8). These are also well matched with earlier published data (Ertl et al., 2002, Frank-Kamenetskaya &
281 Rozhdestvenskaya, 2004). Values of $\Delta_{\text{oct}}Z$ distortion for all the investigated tourmalines are almost the
282 same, which is well explained by the similarity in chemical composition of the Z-octahedra. The value
283 of T-site distortion is almost insignificant, and reaches its maximum in copper-bearing olenite, where it
284 can be explained by the maximum Al cation content in the T-site.

285

286 **Conclusion**

287

288 The crystal-chemical regularities of tourmalines with copper admixture ranging from 0.38 to 8.39
289 wt.% CuO were analyzed. The maximum value of copper content in natural Cu-bearing elbaïtes (Paraiba
290 occurrence) was 3.59 wt. % CuO, which can be related to the specific conditions of mineral formation.

291 Copper and other 3d element cations (Mn, Zn, Fe) almost only occupy the Y octahedron. Such
292 ordering distribution of copper cations is well explained by the Goldschmidt rule.

293 The entry of copper and other 3d elements increases the parameters of the tourmaline unit cell
294 and the sizes of Y-octahedra. As the site scattering and size of Z octahedron is almost similar, the
295 difference between the size of the Y and Z octahedra is increasing with increasing Cu content. Our
296 results indicate that very small amounts of Cu also occupy the Z site (<4%). However, for a final proof
297 of these refinement results spectroscopic investigations would be necessary.

298 Values of polyhedron distortion in structures of copper-bearing elbaïte are close to each other, but
299 significantly higher than in the structure of copper-bearing olenite.

300 Additional studies of synthetic Cu-rich tourmaline, especially focusing on the tetrahedral
301 positions are now in progress.

302 **Acknowledgements**

303

304 The authors thank L.G. Kuznetsova for help in lithium determination. We also are grateful to
305 reviewers Andreas Ertl and Barb Dutrow, and editor Darby Dyar, for many helpful discussions which
306 improved the manuscript.

307 This work was supported by the Russian Foundation for Basic Research (project 09-05-00769-
308 a).

309

309 **References:**

310

311 Abduriyim, A., Kitawaki, H., Furuya, M., Schwarz, D. (2006) "Paraiba"-type copper-bearing
312 tourmaline from Brazil, Nigeria, and Mozambique: Chemical fingerprinting by LA-ICP-MS. *Gems &*
313 *Gemology*, 42, 1, 4-21.

314 Abduriyim, A., Kitawaki, H. (2005) Cu- and Mn-bearing tourmaline: More production from
315 Mozambique. *Gems & Gemology*, 41, 4, 360-361.

- 316 Akselrud, L.G., Grin, Yu.N., Zavalij, P.Yu., Pecharsky, V.K., Fundamenskii, V.S. (1989) CSD
317 - Universal program package for single crystal and/or powder structure data treatment. 12-th European
318 crystallographic meeting: Abstract of papers, Moscow, 3, 155.
- 319 Bank, H., Henn, U., Bank, F.H., von Platen, H., Hofmeister, W. (1990) Leuchtendblaue Cu-
320 führende Turmaline aus Paraiba, Brasilien. Zeitschrift der Deutschen Gemmologischen Gesellschaft,
321 39, 1, 3-11.
- 322 Bank, H., Henn, U. (1990) Paraiba tourmaline: Beauty and rarity. Jewellery News Asia, 70, 62,
323 64.
- 324 Bassett, H. (1953) A vanadiferous variety of tourmaline from Tanganyika. Record of
325 Geological Survey of Tanganyika, 93-96.
- 326 Bettencourt, D.M., Wilson, W.E. (2000) Famous mineral localities: The Alto Ligonha
327 pegmatites, Mozambique. Mineralogical Record, 31, 459-497.
- 328 Breeding, C.M., Rockwell, K., Laurs, B.M. (2007) Gem news international: New Cu-bearing
329 tourmaline from Nigeria. Gems & Gemology, 43, 4, 384-385.
- 330 Beurlen, H. et al. (2011) Geochemical and geological controls on the genesis of gem-quality
331 "Paraiba tourmaline" in granitic pegmatites from northeastern Brazil, Canadian Mineralogist, 49, 277-
332 300
- 333 Bosi, F., Lucchesi, S., Reznitskii, L. (2004) Crystal chemistry of the dravite-chromdravite
334 series, European Mineralogical Journal, 16, 2, 345-352
- 335 Bosi, F., Andreozzi, G. B., Federico, M., Graziani, G., and Lucchesi, S. (2005) Crystal
336 chemistry of the elbaite-schorl series, American Mineralogist, 90, 1784-1792
- 337 Bosi, F., Lucchesi, S. (2007) Crystal chemical relationships in the tourmaline group: Structural
338 constraints on chemical variability, American Mineralogist, 92, 1054-1063
- 339 Burns, P.C., MacDonald, J., Hawthorne, F.C. (1994) The crystal chemistry of manganese-
340 bearing elbaite, The Canadian Mineralogist, 32, 31-42
- 341 Cempírek, J., Novák, M., Ertl, A., Hughes, J.M., Rossman, G.R., Dyar, M.D. (2006) Fe-bearing
342 olenite with tetrahedrally coordinated Al from an abyssal pegmatite at Kutná Hora, Czech republic:
343 structure, crystal chemistry, optical and xanes spectra. The Canadian Mineralogist, 44, 23-30
- 344 Ertl, A., Hughes, J.M., Pertlik, F., Foit, F.F., Jr., Wright, S.E., Brandstätter, F., Marler, B.
345 (2002) Polyhedron distortions in tourmaline, The Canadian Mineralogist, 40, 153-162.
- 346 Ertl, A., Hughes, J.M., Prowatke S., Rossman G.R., London D., Fritz, E.A. (2003) Mn-rich
347 tourmaline from Austria: structure, chemistry, optical spectra and relations to synthetic solid solutions,
348 American Mineralogist, 88, 1369-1376
- 349 Ertl, A., Mali, H., Schuster, R., Körner, W., Hughes, J.M., Brandstätter, F. & Tillmanns, E.
350 (2010): Li-bearing, disordered Mg-rich tourmalines from the pegmatite-marble contact from the
351 Austroalpine basement units (Styria, Austria). Mineralogy and Petrology, 99, 89-104.
- 352 Ertl, A. & Tillmanns, E. (2012) The [9]-coordinated X site in the crystal structure of
353 tourmaline-group minerals. Z. Krist., 227, 456-459
- 354 Frank-Kamenetskaya, O.V. and Rozhdestvenskaya, I.V. (2004) Atomic defects and crystal
355 structure of minerals. Ch. III. Advances in science and technics. Crystal chemistry; Saint-Petersburg.
356 Yanus, 55-70.
- 357 Furuya, M., Furuya, M. (2007) Paraiba Tourmaline-Electric Blue Brilliance Burnt into Our
358 Minds. Japan Germany Gemmological Laboratory, Kofu, Japan, 24
- 359 Goldschmidt, V.M. (1933) The main geochemistry concepts Fersman, A.V ed. Moscow,
360 Goschimtextisdat (in Russian).
- 361 Gorskaya, M.G., Frank-Kamenetskaya, O.V., Rozhdestvenskaya I.V., Frank-Kamenetskiy,
362 V.A. (1982) The refinement of crystal structure Al- rich elbaite, Crystallography, 27, 1, 107-112 (in
363 Russian)
- 364 Haughton, S. H., (1969) Geological history of Southern Africa. Geological Society of South
365 Africa, Cape Town, 535
- 366 Hawthorne, F.C. (1996): Structural mechanisms for light-element variations in tourmaline. The
367 Canadian Mineralogist, 34, 123-132

- 368 Hawthorne, F.C. (2002): Bond-valence constraints on the chemical composition of tourmaline.
369 *The Canadian Mineralogist*, 40, 789-797
- 370 Henn, U. and Bank, H. (1990) Origin the colour and pleochroism of Cu-bearing green and blue
371 tourmalines from Paraiba, Brazil. *Neues Jahrbuch für Mineralogie, Monatshefte*, 6, 280–288
- 372 Henricus, J. (2001) New Nigeria tourmaline find excites trade interest. *Jewellery News Asia*,
373 207, 77-78, 87
- 374 Henry, D.J., Novak, M., Hawthorne, F.C., Ertl, A., Dutrow, B., Uher, P. and Pezzotta, F. (2011)
375 Nomenclature of the tourmaline-supergroup minerals. *American Mineralogist*, 96, 895–913
- 376 Koivula, J. I., Nagle, K., Shen, A. H-T., Owens, P. (2009) Solution-generated pink color
377 surrounding growth tubes and cracks in blue to blue-green copper-bearing tourmalines from
378 Mozambique. *Gems & Gemology*, 40, 1, 44-47
- 379 Laurs, B.M., Zwaan, J.C., Breeding, C.M., Simmons, W.B., Beaton, D., Rijdsdijk, K.F., Befi, R.,
380 Falster, A.U. (2008) Copper-bearing (Paraiba-type) tourmaline from Mozambique. *Gems & Gemology*
381 44, 1, 4-30
- 382 Lächelt, S. (2004) The geology and mineral resources of Mozambique. National Directorate of
383 Geology, Maputo, Mozambique, 515
- 384 Lebedev, A.S., Kargalcev, S.V., Pavlychenko, V.S. (1988) Synthesis and properties of
385 tourmaline series Al-Mg-(Na) and Al-Fe-(Na). In proceedings of genetic and experimental mineralogy.
386 Growth and properties of crystals. Novosibirsk, Nauka. (in Russian)
- 387 MacDonald, D.J. and Hawthorne, F.C. (1995) Cu-bearing tourmaline from Paraiba, Brazil,
388 *Acta Crystallographica*, 51, 555-557
- 389 Mashkovtsev, R.I., Smirnov, S.Z. and Shigley, J. E. (2006) The features of the Cu²⁺- entry into
390 the structure of tourmaline, *Journal of Structural Chemistry*. 47, 2, 252-257
- 391 Peretti, A., Bieri, W.P., Reusser, E., Hametner, K., and Günther D. (2009) Chemical variations
392 in multicolored “Paraiba”-type tourmalines from Brazil and Mozambique: Implications for origin and
393 authenticity determination”. *Contributions to Gemology, Gem Research Swiss Lab. No. 9*. 76 pages
- 394 Power, G.M. (1968): Chemical variation in tourmalines from south–west England.
395 *Mineralogical Magazine*, 36, 1078-1089
- 396 Rossman, G. et al. (1991) Origin of color in cuprian elbaite from Sao Jose de Batalha, Paraiba,
397 Brazil, *American Mineralogist*, 76, 1479-1484
- 398 Rozhdestvenskaya, I.V. et al. (2005) Refinement of the crystal structures of three fluorine-
399 bearing elbaite, *Crystallography Reports*, 50, 6, 907–913
- 400 Shigley, J. E., Cook, B. C., Laurs, B. M., Bernardes, O. M. (2001) An update on "Paraiba"
401 tourmaline from Brazil. *Gems & Gemology*, 37, 4, 260-276
- 402 Schmetzer, K., Nuber, B., Abraham, K. (1979) Zur Kristallchemie Magnesium-reicher
403 Turmaline. *Neues Jahrbuch für Mineralogie*, 136, 1, 93-112
- 404 Sokolov, P.B., Gorskaya, M.G., Gordienko, V.V., Petrova, M.G., Kretser, Yu.L. & Frank-
405 kamenetskii, V.A. (1986) Olenite, NaAl₃Al₆B₃Si₆O₂₇(O,OH)₄ – a new high-alumina mineral of the
406 tourmaline group. *Notes of Mineralogical Society*, 115, 119-123 (in Russian)
- 407 Taran, M.N., Lebedev, A.S., Platonov, A.N. (1993) Optical Absorption Spectroscopy of
408 Synthetic Tourmalines, *Physics and Chemistry of Minerals*, 20, 3, 209-220
- 409 Vereshchagin, O.S., Rozhdestvenskaya, I.V., Frank-Kamenetskaya, O.V., Zolotarev, A.A.
410 (2010) Crystal chemistry and the nomenclature of chromium-bearing tourmalines. CD of Abstracts the
411 20-th General Meeting of the International Mineralogical Association, Budapest, Hungary, 710.
- 412 Voskresenskaya, I.E., Barsukova, M.L., (1968) In *Hydrothermal synthesis of crystals*, Moscow,
413 Nauka (in Russian)
- 414 Walker, N., Stuart, D., (1983) An empirical method for correcting diffractometer data for
415 absorption effects. *Acta Crystallographica*, A39, 158-166
- 416 Wilson, W. (2002) Cuprian elbaite from the Batalha Mine, Paraiba, Brazil, *Mineralogical*
417 *Record*, 33
- 418 Wise, R.W. (2007) Mozambique: The new Paraiba Colored Stone, 20, 2, 10-11

- 419 Wright, S.E., Foley, J.A., and Hughes, J.M. (2000) Optimization of site occupancies in
420 minerals using quadratic programming. *American Mineralogist*, 85, 524-531
- 421 Zang, J.W., Da Fonseca-Zang, W. A., Fliss, F., Höfer, H. E., Lahaya, Y. (2001) Cu-haltige
422 Elbaite aus Nigeria. *Berichte der Deutschen Mineralogischen Gesellschaft, Beihefte zum European*
423 *Journal of Mineralogy*, 13, 202
- 424 Zolotarev, A.A., Frank-Kamenetskaya, O.V., Rozhdestvenskaya, I.V. (2007) Crystalchemical
425 formulas and definition of species of tourmaline - group minerals. *Geology of Ore Deposits*, 49, 7, 547

Table 1. Characteristics of examined tourmalines

<i>Smp.</i>	<i>Origin/Occurrence</i>	<i>Crystal description</i>
1	Synthetic	Fragments of the crystal, size up to 0.6 mm, colored blue.
2	Paraiba, Brasil	Elongated, up to 1 cm zone-colored crystals, the internal parts colored blue, border – purple.
3		

Table 2. Parameters of X-ray data collection and unit cell parameters of the examined tourmalines

<i>Characteristic</i>	<i>Samples</i>		
	<i>1</i>	<i>2</i>	<i>3</i>
Size smp. (mm)	0.10*0.10*0.10	0.10*0.05*0.10	0.10*0.15*0.10
Diffractometer	Nicolett R3	Bruker APEX2	Nicolett R3
Scan mode, detector	ω - scan mode, V = 2-30 degree /min, scintillation detector	CCD camera	ω - scan mode, V = 2-30 degree /min, scintillation detector
$2\theta_{\max}$	80.00°	71.80°	80.00°
Measured reflections $I > 2\sigma_I$	2289	9289	3201
$F_{\text{obs}}^{\text{un.}} > 4.0\sigma_F$	1153	890	1152
$R_{\text{sig}}/R_{\text{eq}}$	0.039/0.045	0.005/ 0.038	0.029/ 0.034
R/R_w	0.041/0.045	0.022/ 0.025	0.031/ 0.033
GOF	0.91	0.96	1.03
$a, \text{Å}$	15.840(4)	15.881(1)	15.840(3)
$c, \text{Å}$	7.091(1)	7.112(1)	7.1028(9)

Note. Here and in Tables 3–5 the sample numbers are those of Table 1

Table 3. Chemical compositions of examined tourmalines (wt. %) and coefficients in the formula $X_{0-1}Y_3Z_6(T_6O_{18})(BO_3)_3V_3W$

Component	Sample		
	1	2	3
SiO ₂	30.84	36.65	37.68
Al ₂ O ₃	43.10	37.27	41.32
CuO	8.39	3.59	1.46
FeO	0.00	0.26	0.00
ZnO	0.00	2.30	0.00
Mn ₂ O ₃	0.00	1.38	1.11
Li ₂ O*	0.00	1.62	1.97
CaO	0.00	0.16	0.52
Na ₂ O	3.22	2.79	1.99
F	0.00	0.43	0.49
B ₂ O ₃ (calc)	12.71	10.75	11.15
H ₂ O (calc)	0.47	3.50	3.61
Sum	98.73	100.69	101.29

Site	Component	Sample		
		1	2	3
T	Si	5.26	5.93	5.87
	Al	0.74	0.07	0.13
	Sum	6.00	6.00	6.00
Y + Z	Al	7.92	7.03	7.46
	Cu	1.08	0.44	0.17
	Fe	0.00	0.03	0.00
	Zn	0.00	0.27	0.00
	Mn	0.00	0.17	0.13
	Li*	0.00	1.05	1.24
Sum	9.00	9.00	9.00	
X	Ca	0.00	0.03	0.09
	Na	1.06	0.87	0.60
	Sum	1.06	0.90	0.69
V+W	O	1.00	0.00	0.00
	OH	3.00	3.78	3.76
	F	0.00	0.22	0.24
	Sum	4.00	4.00	4.00

Note: * Li₂O content was calculated from the charge balance. In Sample 2 the lithium content was obtained by calculation, and is close to that obtained by the flame photometry method at the Institute of Geochemistry SB RAS, Irkutsk, Russia, by L.G. Kuznetsova.

Table 4. Typical chemical compositions of Paraíba tourmalines (wt. %)

	Peretti, A et al., 2009		Beurlen, H. et al., 2011
	ICP MS	EMPA	EMPA
	Blue zone	Average	05-3a
SiO ₂	37.86	37.74	38.48
Al ₂ O ₃	39.69	41.77	41.08
CuO	1.23	0.55	1.80
FeO	0.00	0.08	0.03
ZnO	0.04	0.07	0.00
Mn ₂ O ₃	1.06	0.45	0.46
Li ₂ O	2.15	-	2.01
CaO	0.30	0.13	0.67
Na ₂ O	2.00	1.83	1.98
Bi ₂ O ₃	0.11	0.13	0.09
K ₂ O	0.01	0.02	0.02
Ga ₂ O ₃	0.01	-	-
F	-	0.72	1.46
H ₂ O	-	-	3.18
B ₂ O ₃	12.07	11	11.21
Sum	96.53	94.49	101.85

Table 5. The site scattering, atom coordinates and isotropic displacement parameters in the crystal structures of the tourmalines investigated

Site	Smp.	Site scattering, e per site	<i>x/a</i>	<i>y/b</i>	<i>z/c</i>	$U_{is/eq}^* \cdot 100, \text{\AA}^{-2}$
X 3a	1	9.57(2)	0	0	0.2186(9)	2.3(1)
	2	10.50(1)	0	0	0.2350(4)	2.42(6)
	3	8.95(2)	0	0	0.2348(6)	1.90(10)
Y 9b	1	19.08(1)	0.12342(7)	1/2x	0.6347(2)	0.73(2)
	2	14.32(1)	0.12456(5)	1/2x	0.6305(1)	0.81(2)
	3	10.60(1)	0.1234(1)	1/2x	0.6332(2)	0.65(3)
Z 18c	1	13.32(1)	0.29747(7)	0.26001(7)	0.6055(2)	0.53(3)
	2	13.83(1)	0.29773(4)	0.26045(4)	0.6109(1)	0.67(2)
	3	13.48(1)	0.29688(5)	0.26004(5)	0.6095(1)	0.57(2)
T 18c	1	13.90(1)	0.19206(6)	0.18989(6)	0.00000	0.44(2)
	2	13.95(1)	0.19208(3)	0.19001(3)	0.00000	0.40(1)
	3	13.95(1)	0.19197(4)	0.18979(4)	0.00000	0.33(2)
B 9b	1	5.00	0.1092(2)	2x	0.4525(6)	0.41(10)
	2	5.00	0.10899(8)	2x	0.4564(3)	0.57(6)
	3	5.00	0.1091(1)	2x	0.4545(5)	0.45(2)
W1(O1)3a	1	8.00	0	0	0.772(2)	3.3(3)
	2	6.56(3)	0	0	0.7873(8)	4.7(3)
	3	6.64(2)	0	0	0.7773(13)	2.7(2)
W2(F) 9b	1	-	-	-	-	-
	2	1.62(3)	0.0357(9)	1/2x	0.796(2)	2.38(2)
	3	1.71(2)	0.030(1)	1/2x	0.799(3)	3.6(5)
O2 9b	1	8.00	0.0599(1)	2x	0.4922(5)	0.68(8)
	2	8.00	0.06050(7)	2x	0.4893(3)	1.47(6)
	3	8.00	0.06033(9)	2x	0.4887(4)	1.33(7)
O3(V) 9b	1	8.00	0.2627(4)	1/2x	0.5059(6)	1.7(2)
	2	8.00	0.2692(2)	1/2x	0.5079(3)	1.11(5)
	3	8.00	0.2653(2)	1/2x	0.5078(3)	1.10(8)
O4 9b	1	8.00	0.0942(2)	2x	0.0738(6)	1.09(10)
	2	8.00	0.09309(7)	2x	0.0723(3)	0.79(4)
	3	8.00	0.0937(1)	2x	0.0733(4)	0.73(6)
O5 9b	1	8.00	0.1869(3)	1/2x	0.0975(5)	1.05(10)
	2	8.00	0.1861(1)	1/2x	0.0952(3)	0.84(5)
	3	8.00	0.1871(2)	1/2x	0.0956(3)	0.71(6)
O6 18c	1	8.00	0.1954(2)	0.1836(2)	0.7719(4)	0.64(7)
	2	8.00	0.19719(8)	0.18614(9)	0.7750(2)	0.67(3)
	3	8.00	0.1955(1)	0.1848(1)	0.7743(2)	0.60(5)
O7 18c	1	8.00	0.2877(2)	0.2867(2)	0.0746(4)	0.65(7)
	2	8.00	0.28616(8)	0.28592(8)	0.0796(2)	0.60(3)
	3	8.00	0.2865(1)	0.2860(1)	0.0785(2)	0.51(4)
O8 18c	1	8.00	0.2087(2)	0.2687(2)	0.4352(4)	0.59(6)
	2	8.00	0.20945(9)	0.26984(9)	0.4407(2)	0.68(4)
	3	8.00	0.2094(1)	0.2697(1)	0.4386(3)	0.59(4)
H	1	1.00	0.2760(12)	1/2x	0.428(2)	5.2(5)
	2	1.00	0.305(4)	1/2x	0.397(8)	5.1(5)
	3	1.00	0.2629(9)	1/2x	0.3996(7)	9.1(8)

Note: * $U_{eq} = 1/3[U_{11} a^{*2} a^2 + \dots + 2U_{23} b^* c^* bc \cos\alpha]$

Table 6. Bond lengths (Å) in the crystal structures of the tourmalines investigated

Atoms	Samples		
	1	2	3
X - O2 [3]	2.542(7)	2.457(3)	2.448(4)
- O4 [3]	2.782(5)	2.810(2)	2.815(3)
- O5 [3]	2.703(7)	2.746(3)	2.751(5)
average	2.676	2.671	2.671
Y - W1 [1]	1.954(7)	2.044(4)	1.979(6)
- O2 [2]	1.951(5)	1.965(2)	1.964(4)
- O3v [1]	2.118(8)	2.172(3)	2.140(5)
- O6 [2]	1.943(4)	1.997(2)	1.971(4)
average	1.977	2.024	1.998
Y- W2	-	1.70(4)	1.74(2)
Z - O3v [1]	1.958(7)	1.957(3)	1.958(4)
- O6 [1]	1.874(5)	1.849(2)	1.859(3)
- O7 [1]	1.935(4)	1.951(2)	1.946(3)
- O7 [1]	1.875(4)	1.881(2)	1.883(3)
- O8 [1]	1.910(5)	1.914(2)	1.905(3)
- O8 [1]	1.892(5)	1.884(2)	1.887(4)
average	1.907	1.906	1.906
T - O4 [1]	1.625(5)	1.626(3)	1.624(3)
- O5 [1]	1.641(4)	1.641(3)	1.635(4)
- O6 [1]	1.623(4)	1.605(2)	1.607(3)
- O7 [1]	1.614(5)	1.612(2)	1.611(4)
average	1.625	1.621	1.619
B - O2 [1]	1.383(5)	1.354(2)	1.360(3)
- O8 [2]	1.370(6)	1.386(3)	1.380(4)
average	1.375	1.375	1.373
H - O3v	0.58(1)	0.93(6)	0.77(1)
H - O5	2.64(1)	2.70(6)	2.40(1)
W1-W2	-	0.50(2)	0.44(2)
W2-W2	-	0.85(3)	0.72(3)

Table 7. Chemical characteristics of Cu-bearing tourmalines

<i>N</i> <i>o</i>	CuO, wt. %	<i>Crystal chemical formula</i>	<i>Reference</i>
1	8.39	(Na _{0.86} □ _{0.14})(Al _{1.86} Cu _{1.14})(Al _{5.88} Cu _{0.12})(Si _{5.40} Al _{0.60})O ₁₈ × (BO ₃) ₃ ((OH) _{3.00} O)	<i>Our date (Smp.1)</i>
2	3.59	(Na _{0.90} Ca _{0.03} □ _{0.07})(Al _{1.50} Li _{0.75} [Cu,Zn] _{0.54} Mn _{0.18} Fe _{0.03})× (Al _{5.85} [Cu,Zn] _{0.15})(Si _{5.65} Al _{0.32})O ₁₈ (BO ₃) ₃ ((OH) _{3.82} F _{0.18})	<i>Our date (Smp.2)</i>
3	1.46	(Na _{0.65} Ca _{0.09} □ _{0.26})(Al _{1.63} Li _{1.07} Mn _{0.30})(Al _{5.81} Cu _{0.19})(Si _{5.70} Al _{0.30}) O ₁₈ × (BO ₃) ₃ ((OH) _{3.83} F _{0.17})	<i>Our date (Smp.3)</i>
4	0.94	(Na _{0.54} Ca _{0.11} □ _{0.35})(Al _{1.62} Li _{1.13} Cu _{0.11} Mn _{0.08})(Al _{5.91} □ _{0.09})× (Si _{5.74} B _{0.26})O ₁₈ (BO ₃) ₃ ((OH) _{3.61} F _{0.39})	Ertl et al., 2002
5	0.81	(Na _{0.54} Ca _{0.05} □ _{0.41})(Al _{1.66} Li _{1.21} Cu _{0.10} Mn _{0.04})Al _{6.00} ((Si _{5.92} Al _{0.08})O ₁₈)× (BO ₃) ₃ ((OH) _{3.56} F _{0.44})	MacDonald & Hawthorne, 1995
6	0.38	(Na _{0.55} Ca _{0.11} □ _{0.34})(Al _{1.71} Li _{1.16} Cu _{0.05} Mn _{0.08})Al _{6.00} ((Si _{5.88} Al _{0.12})O ₁₈)× (BO ₃) ₃ ((OH) _{3.70} F _{0.30})	
7	0	(Na _{0.68} Ca _{0.22} □ _{0.10})(Li _{1.56} Al _{1.44})(Al _{5.82} Mn _{0.18})(Si ₆ O ₁₈)(BO ₃) ₃ × ((OH) _{3.64} F _{0.36})	Rozhdestvenskaya <i>et al.</i> , 2005

Table 8. Geometric characteristics of Cu-bearing tourmalines

<i>No</i>	<i>a</i> , Å	<i>c</i> , Å	<Y-O>, Å	<Z-O>, Å	<T-O>, Å	ΔX^* 10^3	$\Delta_{\text{oct}Y}$ $*10^3$	$\Delta_{\text{oct}Z}$ $*10^3$	ΔT^* 10^3
1	15.840(4)	7.091(1)	1.978	1.907	1.625	2.07	0.37	0.43	0.15
2	15.881(1)	7.112(1)	2.024	1.906	1.621	3.31	1.25	0.42	0.07
3	15.840(3)	7.1028(9)	1.999	1.906	1.619	3.59	1.05	0.34	0.05
4	15.8308(32)	7.0957(8)	1.998	1.905	1.619	3.50	1.06	0.35	0.05
5	15.818(2)	7.087(1)	1.992	1.904	1.617	3.18	0.98	0.36	0.06
6	15.805(2)	7.084(1)	1.987	1.903	1.616	3.21	1.05	0.36	0.05
7	15.826(3)	7.098(1)	1.996	1.907	1.618	3.71	1.35	0.34	0.08

Note: *a*, *c* – unit cell parameters; <Y-O>, <Z-O>, <T-O> - average polyhedron sizes; ΔX , $\Delta_{\text{oct}Y}$, $\Delta_{\text{oct}Z}$, ΔT – bond-length distortion

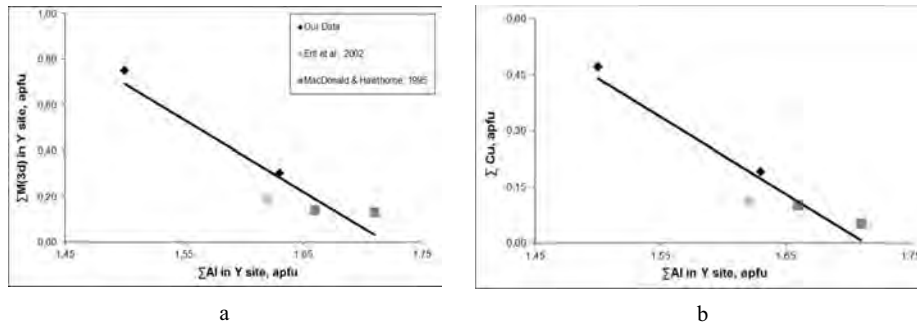


Fig. 1. Content of Al^{3+} cations in Y-octahedron of copper-bearing elbaïtes vs their content of 3d elements (a) and their overall copper content (b).

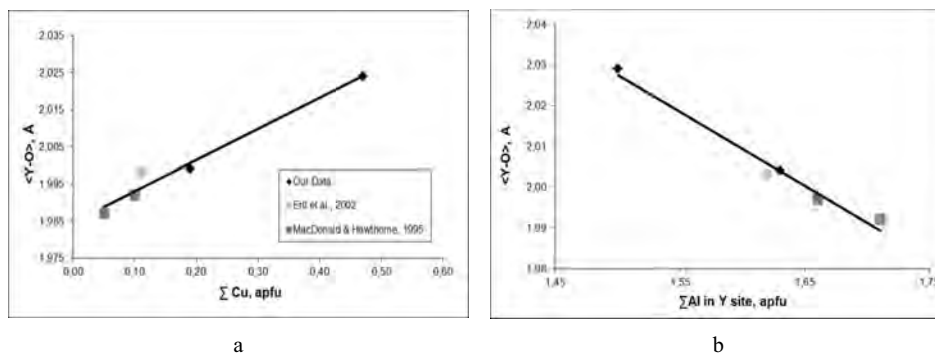


Fig. 2. The value of $\langle Y-O \rangle$ in copper-bearing elbaïtes vs their total contents of Cu^{2+} (a) and Al^{3+} in the Y-octahedron (b).

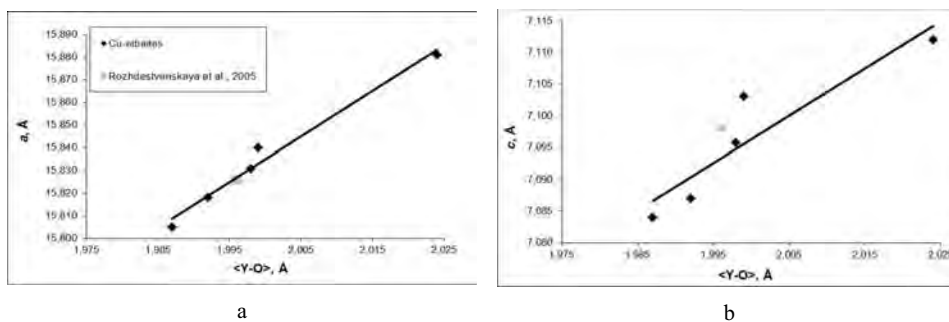


Fig. 3. The value of $\langle Y-O \rangle$ in copper-bearing elbaïtes vs unit cell parameters: a (a) and c (b).